

Measurement of the lifetime of the $B+c$ meson using the $B+c \rightarrow J/\psi \pi^+$ decay mode

J. Aaij, L. Beaucourt, M. Chefdeville, D. Decamp, N. Déleage, Ph. Ghez, J.-P. Lees, J.F. Marchand, M.-N. Minard, B. Pietrzyk, et al.

► To cite this version:

J. Aaij, L. Beaucourt, M. Chefdeville, D. Decamp, N. Déleage, et al.. Measurement of the lifetime of the $B+c$ meson using the $B+c \rightarrow J/\psi \pi^+$ decay mode. *Physics Letters B*, Elsevier, 2015, 742, pp.29-37. <10.1016/j.physletb.2015.01.010>. <in2p3-01088069>

HAL Id: in2p3-01088069

<http://hal.in2p3.fr/in2p3-01088069>

Submitted on 26 Feb 2015

HAL is a multi-disciplinary open access archive for the deposit and dissemination of scientific research documents, whether they are published or not. The documents may come from teaching and research institutions in France or abroad, or from public or private research centers.

L'archive ouverte pluridisciplinaire **HAL**, est destinée au dépôt et à la diffusion de documents scientifiques de niveau recherche, publiés ou non, émanant des établissements d'enseignement et de recherche français ou étrangers, des laboratoires publics ou privés.



Measurement of the lifetime of the B_c^+ meson using the $B_c^+ \rightarrow J/\psi\pi^+$ decay mode



LHCb Collaboration

ARTICLE INFO

Article history:

Received 26 November 2014
 Received in revised form 19 December 2014
 Accepted 9 January 2015
 Available online 13 January 2015
 Editor: M. Doser

ABSTRACT

The difference in total widths between the B_c^+ and B^+ mesons is measured using a data sample corresponding to an integrated luminosity of 3.0 fb^{-1} collected by the LHCb experiment in 7 and 8 TeV centre-of-mass energy proton–proton collisions at the LHC. Through the study of the time evolution of $B_c^+ \rightarrow J/\psi\pi^+$ and $B^+ \rightarrow J/\psi K^+$ decays, the width difference is measured to be

$$\Delta\Gamma \equiv \Gamma_{B_c^+} - \Gamma_{B^+} = 4.46 \pm 0.14 \pm 0.07 \text{ mm}^{-1} c,$$

where the first uncertainty is statistical and the second systematic. The known lifetime of the B^+ meson is used to convert this to a precise measurement of the B_c^+ lifetime,

$$\tau_{B_c^+} = 513.4 \pm 11.0 \pm 5.7 \text{ fs},$$

where the first uncertainty is statistical and the second is systematic.

© 2015 The Authors. Published by Elsevier B.V. This is an open access article under the CC BY license (<http://creativecommons.org/licenses/by/4.0/>). Funded by SCOAP³.

1. Introduction

For weakly decaying beauty hadrons the heavy quark expansion [1–4] predicts lifetime differences of the order $(\Lambda_{\text{QCD}}/m_b)$, where Λ_{QCD} is the scale parameter of the strong interaction and m_b is the b-quark mass. In agreement with the expectations, differences between B^+ , B^0 , B_s^0 , Λ_b^0 , Ξ_b^0 and Ξ_b^- lifetimes not exceeding a few per cent are found experimentally [5–11]. The B_c^+ meson is a bound state of an anti-b quark and a charm quark, and Cabibbo-favoured decays of the charm quark are expected to account for 70% of its total width, resulting in a significantly shorter lifetime than for other B mesons. In addition, non-spectator topologies, in particular annihilation amplitudes, are not Cabibbo-suppressed. These could give sizeable contributions to the total width [12–18]. Understanding the relative contributions of beauty and charm quarks to the total width of the B_c^+ meson is important for predicting the properties of unobserved baryons with two heavy quarks [19,20].

The lifetime of the B_c^+ meson was first measured by the CDF [21–23] and D0 [24] Collaborations using semileptonic $B_c^+ \rightarrow J/\psi\mu^+\nu_\mu X$ and hadronic $B_c^+ \rightarrow J/\psi\pi^+$ decays.¹ The average value of these measurements is $\tau_{B_c^+} = 452 \pm 32 \text{ fs}$ [25]. Recently, the LHCb Collaboration made the most precise measurement to date

of the B_c^+ meson lifetime using semileptonic $B_c^+ \rightarrow J/\psi\mu^+\nu_\mu X$ decays, $\tau_{B_c^+} = 509 \pm 14 \text{ fs}$ [26].

In this Letter we report a measurement of the B_c^+ meson lifetime obtained via the difference between the total width of the B_c^+ and B^+ mesons in the hadronic modes $B_c^+ \rightarrow J/\psi\pi^+$ and $B^+ \rightarrow J/\psi K^+$, using the technique developed in Refs. [7–11,27]. The measurement uses a data sample corresponding to an integrated luminosity of 3.0 fb^{-1} collected by the LHCb experiment in proton–proton (pp) collisions at centre-of-mass energies of 7 and 8 TeV. This study is complementary to the measurement of the B_c^+ lifetime using the semileptonic $B_c^+ \rightarrow J/\psi\mu^+\nu_\mu X$ decays described in Ref. [26].

The B_c^+ lifetime is determined as follows. The decay time distribution for signal, $N_B(t)$, can be described as the product of an acceptance function $\varepsilon_B(t)$ and an exponential decay $E_B(t) = \exp(-t/\tau_B)$ convolved with the decay time resolution of the detector. The effect of the decay time resolution on the ratio $\mathcal{R}(t) \equiv N_{B_c^+}(t)/N_{B^+}(t)$ is found to be small and is absorbed into the ratio of acceptance functions. This leads to the simplified expression

$$\mathcal{R}(t) \propto \frac{\varepsilon_{B_c^+}(t) E_{\tau_{B_c^+}}(t)}{\varepsilon_{B^+}(t) E_{\tau_{B^+}}(t)} \equiv \mathcal{R}_\varepsilon(t) e^{-\Delta\Gamma t}$$

$$\text{with } \Delta\Gamma \equiv \Gamma_{B_c^+} - \Gamma_{B^+} = \frac{1}{\tau_{B_c^+}} - \frac{1}{\tau_B}, \quad (1)$$

¹ The inclusion of charge-conjugate process is implied through this Letter.

where the factor $\mathcal{R}_\varepsilon(t)$ denotes the ratio of the acceptance functions. This allows a precise measurement of $\Delta\Gamma$ and hence of the lifetime of the B_c^+ meson.

2. Detector and event simulation

The LHCb detector [28] is a single-arm forward spectrometer covering the pseudorapidity range $2 < \eta < 5$, designed for the study of particles containing b or c quarks. The detector includes a high-precision tracking system consisting of a silicon-strip vertex detector surrounding the pp interaction region [29], a large-area silicon-strip detector located upstream of a dipole magnet with a bending power of about 4 Tm, and three stations of silicon-strip detectors and straw drift tubes [30] placed downstream of the magnet. The tracking system provides a measurement of momentum, p , with a relative uncertainty that varies from 0.4% at low momentum to 0.6% at 100 GeV/c. The minimum distance of a track to a primary vertex, the impact parameter, is measured with a resolution of $(15 + 29/p_T)$ μm , where p_T is the component of momentum transverse to the beam, in GeV/c. Different types of charged hadrons are distinguished using information from two ring-imaging Cherenkov detectors (RICH) [31]. Photon, electron and hadron candidates are identified by a calorimeter system consisting of scintillating-pad and preshower detectors, an electromagnetic calorimeter and a hadronic calorimeter. Muons are identified by a system composed of alternating layers of iron and multiwire proportional chambers [32].

The trigger [33] comprises two stages. Events are first required to pass the hardware trigger, which selects muon candidates with $p_T > 1.5$ GeV/c or pairs of opposite-sign muon candidates with a requirement that the product of the muon transverse momenta is larger than 1.7 (2.6) GeV^2/c^2 for data collected at $\sqrt{s} = 7$ (8) TeV. The subsequent software trigger is composed of two stages, the first of which performs a partial event reconstruction, while full event reconstruction is done at the second stage. At the first stage of the software trigger the invariant mass of well-reconstructed pairs of oppositely charged muons forming a good two-prong vertex is required to exceed 2.7 GeV/c^2 , and the two-prong vertex is required to be significantly displaced with respect to the reconstructed pp collision vertex.

In the simulation, pp collisions are generated using PYTHIA [34] with a specific LHCb configuration [35]. A dedicated generator, BCVEGPy [36], which implements explicit leading-order matrix element calculations [37–39], is used for production of B_c^+ mesons. The kinematic distributions of B_c^+ mesons are reproduced by the BCVEGPy generator with percent-level precision [26,40–47], while the simulated B^+ samples, produced with PYTHIA, are corrected to reproduce the observed kinematic distributions. Decays of hadronic particles are described by EVTGEN [48], in which final-state radiation is generated using PHOTOS [49]. The interaction of the generated particles with the detector and the detector response are implemented using the GEANT4 toolkit [50] as described in Ref. [51].

3. Event selection

The offline selection of $B_c^+ \rightarrow J/\psi\pi^+$ and $B^+ \rightarrow J/\psi K^+$ candidates is divided into two parts. An initial selection is applied to reduce the combinatorial background. Subsequently, a multivariate estimator based on an artificial neural network algorithm [52,53], configured with a cross-entropy cost estimator [54], in the following referred as MLP classifier, is applied. The same criteria are used for both the B_c^+ and B^+ candidates.

The selection starts from well-identified muon candidates that have a transverse momentum in excess of 550 MeV/c. Pairs of muon candidates are required to form a common vertex and to

have an invariant mass within ± 60 MeV/c^2 of the known J/ψ mass [5]. To ensure that the J/ψ candidate originates in a b-hadron decay, a significant decay length with respect to the pp collision vertex is required. The charged pions and kaons must be positively identified using the combined information from the RICH, calorimeter and muon detectors. The B_c^+ and B^+ candidates are formed from $J/\psi\pi^+$ and $J/\psi K^+$ combinations, respectively. To improve the invariant mass and decay time resolutions for selected candidates, a kinematic fit [55] is applied in which a primary vertex pointing constraint and a mass constraint on the intermediate J/ψ states are applied. To reduce combinatorial background, a requirement on the χ^2 of this fit, χ_{fit}^2 , is imposed and the decay time of the reconstructed B_c^+ (B^+) candidate is required to be in the range $50 < t < 1000$ $\mu\text{m}/c$.

The final selection of candidates using the MLP classifier is based on the transverse momenta and rapidities of reconstructed B_c^+ (B^+) and J/ψ , the transverse momentum and pseudorapidity of the π^+ (K^+) candidate, the cosine of the decay angle θ between the momentum of the π^+ (K^+) in the rest frame of the B_c^+ (B^+) candidate and the boost direction from the B_c^+ (B^+) rest frame to the laboratory frame, the χ^2 of the B_c^+ (B^+) vertex fit, and χ_{fit}^2 . These variables provide good discrimination between signal and background whilst keeping the selection efficiency independent of the B_c^+ (B^+) decay time. The MLP classifier is trained on a simulated sample of $B_c^+ \rightarrow J/\psi\pi^+$ events and a background data sample from the mass sidebands of the B_c^+ signal peak. It is tested on independent samples from the same sources. The working point of the classifier is chosen to minimize $\sigma(\mathcal{S})/\mathcal{S}$, where \mathcal{S} is the B_c^+ signal yield and $\sigma(\mathcal{S})$ is the yield uncertainty, as determined by the mass fit described in the next section. The same MLP classifier is used for the $B^+ \rightarrow J/\psi K^+$ mode.

4. Measurement of $\Delta\Gamma$

The invariant mass distributions for selected B_c^+ and B^+ candidates are presented in Fig. 1. The signal yields are determined using an extended unbinned maximum likelihood fit in which the signal distributions are modelled by a Gaussian function with power-law tails on both sides of the peak [56], and the background is modelled by the product of an exponential and a first-order polynomial function. Simulation studies suggest that the same tail parameters apply for the B_c^+ and B^+ signals. The tail parameters determined from the data for the large B^+ signal are in good agreement with the simulation. The fit gives 2886 ± 71 signal B_c^+ decays and 586065 ± 798 signal B^+ decays. The fitted values for the B_c^+ and B^+ invariant masses are consistent with the known values [5] and the fitted mass resolutions agree with the expectation from simulation.

The signal yields of B_c^+ and B^+ mesons in bins of decay time are shown in Fig. 2(a). A non-uniform binning scheme is chosen with a minimal bin width of 25 $\mu\text{m}/c$ at low t increasing to 200 $\mu\text{m}/c$ at the largest decay times, to keep the B_c^+ signal yield above 20 for all t bins. In the mass fits of the individual decay time bins the peak positions and mass resolutions are fixed to the values obtained from the fit in the entire region, $50 < t < 1000$ $\mu\text{m}/c$.

The decay time resolution function is estimated using simulated samples and found to be well described by triple Gaussian functions with overall rms widths of 10.9 $\mu\text{m}/c$ and 11.5 $\mu\text{m}/c$ for B_c^+ and B^+ decays, respectively. The ratio of acceptance functions, $\mathcal{R}_\varepsilon(t)$, is determined using the simulation and shown in Fig. 2(b). The variation in the acceptance ratio is caused by the requirement on the J/ψ decay length imposed in the trigger and the subsequent selection. The acceptance is calculated as the ratio of decay time distributions of the reconstructed and selected simulated events to the theoretical (exponential) distributions con-

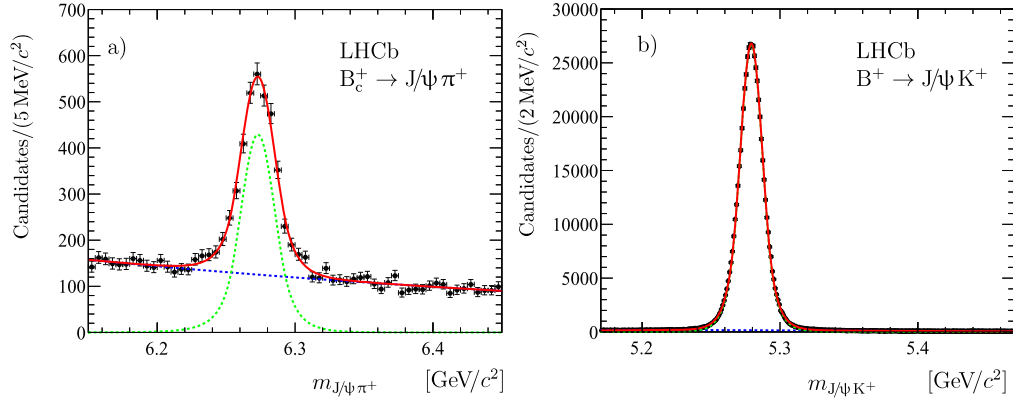


Fig. 1. Invariant mass distributions for (a) selected $B_c^+ \rightarrow J/\psi\pi^+$ and (b) $B^+ \rightarrow J/\psi K^+$ candidates. The fit result with the function described in the text is shown by the red solid line; the signal (background) components are shown with green (blue) dotted lines. (For interpretation of the references to color in this figure legend, the reader is referred to the web version of this article.)

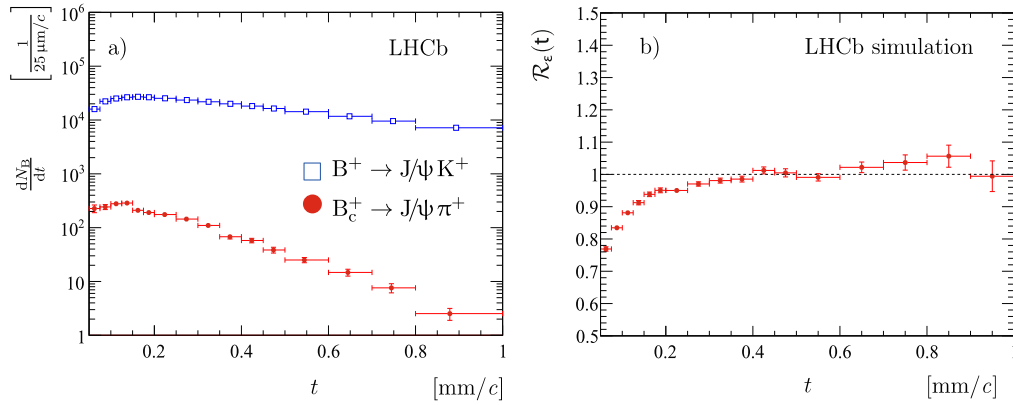


Fig. 2. (a) Decay time distributions for selected $B_c^+ \rightarrow J/\psi\pi^+$ (red solid circles) and $B^+ \rightarrow J/\psi K^+$ (blue open squares) decays, with the data points positioned within the t bins according to Eq. (6) in Ref. [57]; (b) Ratio of acceptance functions $\mathcal{R}_\epsilon(ct)$. The uncertainties are due to sample size only. For visualization purposes the efficiency ratio is normalized as $\mathcal{R}_\epsilon(0.5 \text{ mm}/c) = 1$.

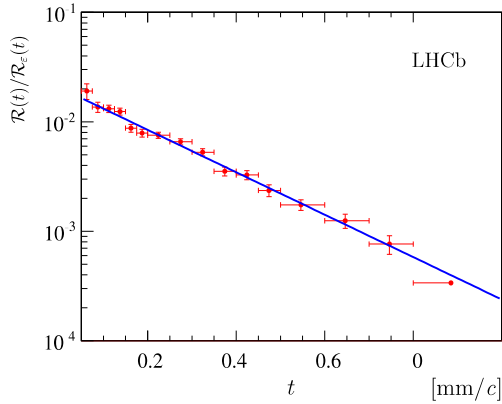


Fig. 3. Ratio of the efficiency-corrected decay time distributions (points with error bars). The curve shows the result of the fit with an exponential function. The data points are positioned within the t bins according to Eq. (6) in Ref. [57] and the horizontal error bars denote the bin widths.

involved with the resolution function. This effectively includes the corrections due to resolution effects, neglected in Eq. (1). It is estimated that any residual bias is smaller than 0.1% in the range $50 < t < 1000 \mu\text{m}/c$.

The efficiency-corrected ratio $\mathcal{R}(t)/\mathcal{R}_\epsilon(t)$ is shown in Fig. 3. A minimum χ^2 fit with an exponential function, according to Eq. (1), gives

$$\Delta\Gamma = 4.46 \pm 0.14 \text{ mm}^{-1} c, \quad (2)$$

Table 1

Summary of systematic uncertainties for $\Delta\Gamma$.

Source	$\sigma_{\Delta\Gamma} [\text{mm}^{-1} c]$
Fit model (signal and background)	0.012
ct fit range	0.040
ct binning	0.016
Acceptance	
Simulation sample size	0.011
MLP filtering	0.025
J/ψ displacement	0.050
Total	0.072

where the uncertainty is statistical. The quality of the fit is good, with a p -value of 42%.

5. Systematic uncertainties and cross-checks

Several sources of systematic uncertainty are considered, as summarized in Table 1 and discussed below.

The uncertainty related to the determination of the signal yields in t bins is estimated by comparing the nominal results with those obtained using different fit models. As an alternative model for the B_c^+ and B^+ signals, a modified Novosibirsk function [58] and a Gaussian function are used. Although the latter provides poor description for the large B^+ sample for all decay time bins and the low-background B_c^+ signal for bins with $t > 150 \mu\text{m}/c$, there is no effect on the determination of $\Delta\Gamma$. For the combi-

natorial background two alternative parameterizations are used: a pure exponential function and a product of an exponential function and a second-order polynomial function. As an additional check, feed-down components from the Cabibbo-suppressed decays $B_c^+ \rightarrow J/\psi K^+$ and $B^+ \rightarrow J/\psi \pi^+$ are added to the fit. The shapes for these components are determined using the simulation, while the yields are allowed to float in the fit. Based on these studies a systematic uncertainty of $0.012 \text{ mm}^{-1} c$ is assigned. Allowing the position and resolution for B_c^+ and B^+ signals to vary in fits to the individual t bins does not affect the value of $\Delta\Gamma$, and no systematic uncertainty is assigned.

The uncertainties due to the choice of t range and the binning scheme are assessed by varying these and comparing all variants that give a statistical uncertainty for $\Delta\Gamma$ below $0.200 \text{ mm}^{-1} c$. Uncertainties of $0.040 \text{ mm}^{-1} c$ and $0.016 \text{ mm}^{-1} c$ are assigned due to the choice of t range and binning scheme.

The efficiency ratio $\mathcal{R}_\varepsilon(t)$ is determined using simulation, following techniques established in Refs. [7–11,27]. The uncertainty for $\mathcal{R}_\varepsilon(t)$ due to the limited size of the simulated sample is estimated to be $0.011 \text{ mm}^{-1} c$ using a simplified simulation.

The result is stable with respect to large variations of the selection criteria, in particular the working points of the MLP classifier and the displacement criterion for the J/ψ vertex. The latter is the only criterion explicitly affecting the lifetime acceptance. The selection criteria are varied, allowing up to a 20% increase in the statistical uncertainty for $\Delta\Gamma$. Variation of the working point of the MLP classifier results in changes of $0.025 \text{ mm}^{-1} c$ in $\Delta\Gamma$. Tightening the J/ψ meson vertex displacement criterion leads to a $0.050 \text{ mm}^{-1} c$ change in $\Delta\Gamma$. These changes are assigned as systematic uncertainties. The result is also stable with respect to the choice of the input variables used in the MLP classifier. An alternative selection using a boosted decision tree [59] is used for comparison with the MLP classifier. The variation of $\Delta\Gamma$ does not exceed a small fraction of its statistical uncertainty, and no additional systematic uncertainty is assigned. The uncertainties due to the momentum scale and the knowledge of the longitudinal coordinate of the LHCb vertex detector are studied in Ref. [6] and found to be negligible. The total systematic uncertainty for $\Delta\Gamma$ is obtained from the sum in quadrature of the individual contributions listed in Table 1.

As a final cross-check, the whole analysis is repeated using a lifetime-unbiased selection, designed to reduce the lifetime dependence of the acceptance. In this selection, instead of the displacement requirements for the J/ψ meson vertex, both at trigger and subsequent selection, a different approach is adopted requiring the transverse momentum of the J/ψ meson to be above $3 \text{ GeV}/c$. All other selection criteria are the same, including the MLP classifier. This selection has almost uniform acceptance as a function of decay time, but a smaller overall efficiency. The value of $\Delta\Gamma$ obtained using this selection is $4.23 \pm 0.20 \text{ mm}^{-1} c$, where the uncertainty is statistical only. The larger statistical uncertainty for this selection is due to the smaller signal yield and significantly larger background level for small ct . The result agrees with the baseline selection.

The results are supported using a pseudoexperiment technique that combines simulation and data. Each pseudoexperiment is constructed from the sample of B^+ candidates (signal and background) from the data, *i.e.* it is the same for all pseudoexperiments; the sample of signal B_c^+ mesons is obtained using the simulation, and the background sample for B_c^+ candidates is generated using a simplified simulation according to the measured background distributions. The sizes of sub-samples are chosen to reproduce the sample sizes and background-to-signal ratios for data. For each pseudoexperiment the mean lifetime of the B_c^+ meson is chosen randomly in the range between 0.6 times and 1.5 times the known B_c^+ meson

lifetime [5]. The whole analysis is performed for each pseudoexperiment and the value of $\Delta\Gamma$ is determined using the same $\mathcal{R}_\varepsilon(t)$ function as for the baseline analysis. In total 1400 pseudoexperiments are used. The value of $\Delta\Gamma$ is found to be unbiased for the entire test interval of B_c^+ meson lifetimes, and the error estimate is reliable.

6. Results and summary

Using a data sample corresponding to an integrated luminosity of 3.0 fb^{-1} collected by the LHCb experiment in pp collisions at 7 and 8 TeV centre-of-mass energies, the difference in total widths between B_c^+ and B^+ mesons is measured to be

$$\Delta\Gamma \equiv \Gamma_{B_c^+} - \Gamma_{B^+} = 4.46 \pm 0.14 \pm 0.07 \text{ mm}^{-1} c,$$

where the first uncertainty is statistical and the second is systematic. Using the known lifetime of the B^+ meson, $\tau_{B^+} = 1.638 \pm 0.004 \text{ ps}$ [5], this is converted into a precise measurement of the B_c^+ meson lifetime,

$$\tau_{B_c^+} = 513.4 \pm 11.0 \pm 5.7 \text{ fs},$$

where in each case the first uncertainty is statistical, and the second is systematic and includes the uncertainty related to the knowledge of the B^+ meson lifetime. This result is in good agreement with the previous LHCb measurement, $\tau_{B_c^+} = 509 \pm 8 \pm 12 \text{ fs}$, obtained using semileptonic $B_c^+ \rightarrow J/\psi \mu^+ \nu_\mu X$ decays [26], and has comparable precision. The uncertainties for these two LHCb measurements are uncorrelated, leading to a combined measurement,

$$\tau_{B_c^+} = 511.4 \pm 9.3 \text{ fs},$$

where the statistical and systematic uncertainties are added in quadrature.

Acknowledgements

We express our gratitude to our colleagues in the CERN accelerator departments for the excellent performance of the LHC. We thank the technical and administrative staff at the LHCb institutes. We acknowledge support from CERN and from the national agencies: CAPES, CNPq, FAPERJ and FINEP (Brazil); NSFC (China); CNRS/IN2P3 (France); BMBF, DFG, HGF and MPG (Germany); INFN (Italy); FOM and NWO (The Netherlands); MNiSW and NCN (Poland); MEN/IFA (Romania); MinES and FANO (Russia); MinEco (Spain); SNSF and SER (Switzerland); NASU (Ukraine); STFC (United Kingdom); NSF (USA). The Tier1 computing centres are supported by IN2P3 (France), KIT and BMBF (Germany), INFN (Italy), NWO and SURF (The Netherlands), PIC (Spain), GridPP (United Kingdom). We are indebted to the communities behind the multiple open source software packages on which we depend. We are also thankful for the computing resources and the access to software R&D tools provided by Yandex LLC (Russia). Individual groups or members have received support from EPLANET, Marie Skłodowska-Curie Actions and ERC (European Union), Conseil général de Haute-Savoie, Labex ENIGMASS and OCEVU, Région Auvergne (France), RFBR (Russia), XuntaGal and GENCAT (Spain), Royal Society and Royal Commission for the Exhibition of 1851 (United Kingdom). We thank A.K. Likhoded and A.V. Luchinsky for fruitful discussions on B_c^+ meson physics.

References

- [1] V.A. Khoze, M.A. Shifman, Heavy quarks, *Sov. Phys. Usp.* 26 (1983) 387.
- [2] I.I. Bigi, N.G. Uraltsev, Gluonic enhancements in non-spectator beauty decays: an inclusive mirage though an exclusive possibility, *Phys. Lett. B* 280 (1992) 271.

- [3] B. Blok, M.A. Shifman, The rule of discarding $1/N_c$ in inclusive weak decays. 1, Nucl. Phys. B 399 (1993) 441, arXiv:hep-ph/9207236;
B. Blok, M.A. Shifman, The rule of discarding $1/N_c$ in inclusive weak decays. 2, Nucl. Phys. B 399 (1993) 459, arXiv:hep-ph/9209289.
- [4] A. Lenz, Lifetimes and HQE, arXiv:1405.3601.
- [5] Particle Data Group, K.A. Olive, et al., Review of particle physics, Chin. Phys. C 38 (2014) 090001.
- [6] LHCb Collaboration, R. Aaij, et al., Measurements of the B^+ , B^0 , B_s^0 meson and Λ_b^0 baryon lifetimes, J. High Energy Phys. 04 (2014) 114, arXiv:1402.2554.
- [7] LHCb Collaboration, R. Aaij, et al., Measurement of the Λ_b^0 baryon lifetime, Phys. Rev. Lett. 111 (2013) 102003, arXiv:1307.2476.
- [8] LHCb Collaboration, R. Aaij, et al., Precision measurement of the ratio of the Λ_b^0 to \bar{B}^0 lifetimes, Phys. Lett. B 734 (2014) 122, arXiv:1402.6242.
- [9] LHCb Collaboration, R. Aaij, et al., Precision measurement of the mass and lifetime of the Ξ_b^0 baryon, Phys. Rev. Lett. 113 (2014) 032001, arXiv:1405.7223.
- [10] LHCb Collaboration, R. Aaij, et al., Measurement of the \bar{B}_s^0 meson lifetime in $D_s^+ \pi^-$ decays, Phys. Rev. Lett. 113 (2014) 172001, arXiv:1407.5873.
- [11] LHCb Collaboration, R. Aaij, et al., Precision measurement of the mass and lifetime of the Ξ_b^- baryon, Phys. Rev. Lett. 113 (2014) 242002, <http://dx.doi.org/10.1103/PhysRevLett.113.242002>, arXiv:1409.8568.
- [12] C.-H. Chang, Y.-Q. Chen, The decays of B_c meson, Phys. Rev. D 49 (1994) 3399.
- [13] S.S. Gershtein, V.V. Kiselev, A.K. Likhoded, A.V. Tkabladze, Physics of B_c^+ mesons, Phys. Usp. 38 (1995) 1, arXiv:hep-ph/9504319.
- [14] M. Beneke, G. Buchalla, The B_c meson lifetime, Phys. Rev. D 53 (1996) 4991, arXiv:hep-ph/9601249.
- [15] P. Colangelo, F. De Fazio, Using heavy quark spin symmetry in semileptonic B_c decays, Phys. Rev. D 61 (2000) 034012, arXiv:hep-ph/9909423.
- [16] V.V. Kiselev, A.E. Kovalsky, A.K. Likhoded, B_c^+ decays and lifetime in QCD sum rules, Nucl. Phys. B 585 (2000) 353, arXiv:hep-ph/0002127;
V.V. Kiselev, A.E. Kovalsky, A.K. Likhoded, B_c^+ meson decays and lifetime within QCD sum rules, Phys. At. Nucl. 64 (2001) 1860.
- [17] C.-H. Chang, S.-L. Chen, T.-F. Feng, X.-Q. Li, The lifetime of B_c^+ meson and some relevant problems, Phys. Rev. D 64 (2001) 014003, arXiv:hep-ph/0007162;
C.-H. Chang, S.-L. Chen, T.-F. Fe, X.-Q. Li, Study of the B_c meson lifetime, Commun. Theor. Phys. 35 (2001) 51, arXiv:hep-ph/0103194.
- [18] V.V. Kiselev, Decays of the B_c meson, arXiv:hep-ph/0308214.
- [19] V.V. Kiselev, A.K. Likhoded, Baryons with two heavy quarks, Phys. Usp. 45 (2002) 455, arXiv:hep-ph/0103169.
- [20] M. Karliner, J.L. Rosner, Baryons with two heavy quarks: masses, production, decays, and detection, arXiv:1408.5877.
- [21] CDF Collaboration, F. Abe, et al., Observation of the B_c meson in $p\bar{p}$ collisions at $\sqrt{s} = 1.8$ TeV, Phys. Rev. Lett. 81 (1998) 2432, arXiv:hep-ex/9805034.
- [22] CDF Collaboration, A. Abulencia, et al., Measurement of the B_c^+ meson lifetime using $B_c^+ \rightarrow J/\psi e^+ \nu$, Phys. Rev. Lett. 97 (2006) 012002, arXiv:hep-ex/0603027.
- [23] CDF Collaboration, T. Aaltonen, et al., Measurement of the B_c^- meson lifetime in the decay $B_c^- \rightarrow J/\psi \pi^-$, Phys. Rev. D 87 (2013) 011101, arXiv:1210.2366.
- [24] D0 Collaboration, V.M. Abazov, et al., Measurement of the lifetime of the B_c^\pm meson in the semileptonic decay channel, Phys. Rev. Lett. 102 (2009) 092001, arXiv:0805.2614.
- [25] Particle Data Group, J. Beringer, et al., Review of particle physics, Phys. Rev. D 86 (2012) 010001, and 2013 partial update for the 2014 edition.
- [26] LHCb Collaboration, R. Aaij, et al., Measurement of the B_c^+ meson lifetime using $B_c^+ \rightarrow J/\psi \mu^+ \nu_\mu X$ decays, Eur. Phys. J. C 74 (2014) 2839, arXiv:1401.6932.
- [27] LHCb Collaboration, R. Aaij, et al., Measurement of the \bar{B}_s^0 effective lifetime in the $J/\psi f_0(980)$ final state, Phys. Rev. Lett. 109 (2012) 152002, arXiv:1207.0878.
- [28] LHCb Collaboration, A.A. Alves Jr., et al., The LHCb detector at the LHC, J. Instrum. 3 (2008) S08005.
- [29] R. Aaij, et al., Performance of the LHCb vertex locator, J. Instrum. 9 (2014) P09007, arXiv:1405.7808.
- [30] R. Arink, et al., Performance of the LHCb outer tracker, J. Instrum. 9 (2014) P01002, arXiv:1311.3893.
- [31] M. Adinolfi, et al., Performance of the LHCb RICH detector at the LHC, Eur. Phys. J. C 73 (2013) 2431, arXiv:1211.6759.
- [32] A.A. Alves Jr., et al., Performance of the LHCb muon system, J. Instrum. 8 (2013) P02022, arXiv:1211.1346.
- [33] R. Aaij, et al., The LHCb trigger and its performance in 2011, J. Instrum. 8 (2013) P04022, arXiv:1211.3055.
- [34] T. Sjöstrand, S. Mrenna, P. Skands, PYTHIA 6.4 physics and manual, J. High Energy Phys. 05 (2006) 026, arXiv:hep-ph/0603175;
T. Sjöstrand, S. Mrenna, P. Skands, A brief introduction to PYTHIA 8.1, Comput. Phys. Commun. 178 (2008) 852, arXiv:0710.3820.
- [35] I. Belyaev, et al., Handling of the generation of primary events in GAUSS, the LHCb simulation framework, in: Nuclear Science Symposium Conference Record (NSS/MIC), IEEE (2010) 1155.
- [36] C.-H. Chang, C. Driouichi, P. Eerola, X.G. Wu, BCVEGPy: an event generator for hadronic production of the B_c^+ meson, Comput. Phys. Commun. 159 (2004) 192, arXiv:hep-ph/0309120;
C.-H. Chang, J.-X. Wang, X.-G. Wu, BCVEGPy 2.0: an upgrade version of the generator BCVEGPy with an addendum about hadroproduction of the P-wave B_c^+ states, Comput. Phys. Commun. 174 (2006) 241, arXiv:hep-ph/0504017;
X.-G. Wu, BCVEGPy and GENXICC for the hadronic production of the doubly heavy mesons and baryons, J. Phys. Conf. Ser. 523 (2014) 012042, arXiv:1307.3344.
- [37] A.V. Berezhnoy, A.K. Likhoded, M.V. Shevlyagin, Hadronic production of B_c^+ mesons, Phys. At. Nucl. 58 (1995) 672, arXiv:hep-ph/9408284.
- [38] K. Kolodziej, A. Leike, R. Rückl, Production of B_c^+ mesons in hadronic collisions, Phys. Lett. B 355 (1995) 337, arXiv:hep-ph/9505298.
- [39] C.-H. Chang, Y.-Q. Chen, G.-P. Han, H.-T. Jiang, On hadronic production of the B_c^+ meson, Phys. Lett. B 364 (1995) 78, arXiv:hep-ph/9408242.
- [40] LHCb Collaboration, R. Aaij, et al., Observation of $B_c^+ \rightarrow J/\psi D_s^+$ and $B_c^+ \rightarrow J/\psi D_s^{*+}$ decays, Phys. Rev. D 87 (2013) 112012, arXiv:1304.4530.
- [41] LHCb Collaboration, R. Aaij, et al., First observation of the decay $B_c^+ \rightarrow J/\psi K^+$, J. High Energy Phys. 09 (2013) 075, arXiv:1306.6723.
- [42] LHCb Collaboration, R. Aaij, et al., Observation of the decay $B_c^+ \rightarrow B_s^0 \pi^+$, Phys. Rev. Lett. 111 (2013) 181801, arXiv:1308.4544.
- [43] LHCb Collaboration, R. Aaij, et al., Observation of the decay $B_c^+ \rightarrow J/\psi K^+ K^- \pi^+$, J. High Energy Phys. 11 (2013) 094, arXiv:1309.0587.
- [44] LHCb Collaboration, R. Aaij, et al., Evidence for the decay $B_c^+ \rightarrow J/\psi 3\pi^+ 2\pi^-$, J. High Energy Phys. 05 (2014) 148, arXiv:1404.0287.
- [45] LHCb Collaboration, R. Aaij, et al., Measurement of the ratio of B_c^+ branching fractions to $J/\psi \pi^+$ and $J/\psi \mu^+ \nu_\mu$, Phys. Rev. D 90 (2014) 032009, arXiv:1407.2126.
- [46] LHCb Collaboration, R. Aaij, et al., First observation of a baryonic B_c^+ decay, Phys. Rev. Lett. 113 (2014) 152003, arXiv:1408.0971.
- [47] LHCb Collaboration, R. Aaij, et al., Measurement of B_c^+ production at $\sqrt{s} = 8$ TeV, Phys. Rev. Lett. (2015), arXiv:1411.2943, submitted for publication.
- [48] D.J. Lange, The EVTGEN particle decay simulation package, Nucl. Instrum. Methods A 462 (2001) 152.
- [49] P. Golonka, Z. Was, PHOTOS Monte Carlo: a precision tool for QED corrections in Z and W decays, Eur. Phys. J. C 45 (2006) 97, arXiv:hep-ph/0506026.
- [50] Geant4 Collaboration, J. Allison, et al., GEANT4 developments and applications, IEEE Trans. Nucl. Sci. 53 (2006) 270;
Geant4 Collaboration, S. Agostinelli, et al., GEANT4: a simulation toolkit, Nucl. Instrum. Methods A 506 (2003) 250.
- [51] M. Clemencic, et al., The LHCb simulation application, GAUSS: design, evolution and experience, J. Phys. Conf. Ser. 331 (2011) 032023.
- [52] W.S. McCulloch, W. Pitts, A logical calculus of the ideas immanent in nervous activity, Bull. Math. Biophys. 5 (4) (1943) 115.
- [53] F. Rosenblatt, The perceptron: a probabilistic model for information storage and organization in the brain, Psychol. Rev. 65 (1958) 386.
- [54] J.-H. Zhong, et al., A program for the Bayesian neural network in the RooFit framework, Comput. Phys. Commun. 182 (2011) 2655, arXiv:1103.2854.
- [55] W.D. Hulsbergen, Decay chain fitting with a Kalman filter, Nucl. Instrum. Methods A 552 (2005) 566, arXiv:physics/0503191.
- [56] LHCb Collaboration, R. Aaij, et al., Observation of J/ψ -pair production in pp collisions at $\sqrt{s} = 7$ TeV, Phys. Lett. B 707 (2012) 52, arXiv:1109.0963.
- [57] G.D. Lafferty, T.R. Wyatt, Where to stick your data points: the treatment of measurements within wide bins, Nucl. Instrum. Methods A 355 (1995) 541.
- [58] BaBar Collaboration, J.P. Lees, et al., Branching fraction measurements of the color-suppressed decays $\bar{B}^0 \rightarrow D^{(*)0} \pi^0$, $D^{(*)0} \eta$, $D^{(*)0} \omega$, and $D^{(*)0} \eta'$ and measurement of the polarization in the decay $\bar{B}^0 \rightarrow D^{*0} \omega$, Phys. Rev. D 84 (2011) 112007, arXiv:1107.5751;
BaBar Collaboration, J.P. Lees, et al., Phys. Rev. D 87 (2013) 039901 (Erratum).
- [59] L. Breiman, J.H. Friedman, R.A. Olshen, C.J. Stone, Classification and Regression Trees, Wadsworth International Group, Belmont, California, USA, 1984.

LHCb Collaboration

R. Aaij⁴¹, B. Adeva³⁷, M. Adinolfi⁴⁶, A. Affolder⁵², Z. Ajaltouni⁵, S. Akar⁶, J. Albrecht⁹, F. Alessio³⁸, M. Alexander⁵¹, S. Ali⁴¹, G. Alkhazov³⁰, P. Alvarez Cartelle³⁷, A.A. Alves Jr.^{25,38}, S. Amato², S. Amerio²², Y. Amhis⁷, L. An³, L. Anderlini^{17,g}, J. Anderson⁴⁰, R. Andreassen⁵⁷, M. Andreotti^{16,f}, J.E. Andrews⁵⁸, R.B. Appleby⁵⁴, O. Aquines Gutierrez¹⁰, F. Archilli³⁸, A. Artamonov³⁵, M. Artuso⁵⁹,

E. Aslanides⁶, G. Auremma^{25,n}, M. Baalouch⁵, S. Bachmann¹¹, J.J. Back⁴⁸, A. Badalov³⁶, C. Baesso⁶⁰, W. Baldini¹⁶, R.J. Barlow⁵⁴, C. Barschel³⁸, S. Barsuk⁷, W. Barter⁴⁷, V. Batozskaya²⁸, V. Battista³⁹, A. Bay³⁹, L. Beaucourt⁴, J. Beddow⁵¹, F. Bedeschi²³, I. Bediaga¹, S. Belogurov³¹, K. Belous³⁵, I. Belyaev^{31,*}, E. Ben-Haim⁸, G. Bencivenni¹⁸, S. Benson³⁸, J. Benton⁴⁶, A. Berezhnoy³², R. Bernet⁴⁰, A. Bertolin²², M.-O. Bettler⁴⁷, M. van Beuzekom⁴¹, A. Bien¹¹, S. Bifani⁴⁵, T. Bird⁵⁴, A. Bizzeti^{17,i}, P.M. Bjørnstad⁵⁴, T. Blake⁴⁸, F. Blanc³⁹, J. Blouw¹⁰, S. Blusk⁵⁹, V. Bocci²⁵, A. Bondar³⁴, N. Bondar^{30,38}, W. Bonivento¹⁵, S. Borghi⁵⁴, A. Borgia⁵⁹, M. Borsato⁷, T.J.V. Bowcock⁵², E. Bowen⁴⁰, C. Bozzi¹⁶, D. Brett⁵⁴, M. Britsch¹⁰, T. Britton⁵⁹, J. Brodzicka⁵⁴, N.H. Brook⁴⁶, A. Bursche⁴⁰, J. Buytaert³⁸, S. Cadeddu¹⁵, R. Calabrese^{16,f}, M. Calvi^{20,k}, M. Calvo Gomez^{36,p}, P. Campana¹⁸, D. Campora Perez³⁸, L. Capriotti⁵⁴, A. Carbone^{14,d}, G. Carboni^{24,l}, R. Cardinale^{19,38,j}, A. Cardini¹⁵, L. Carson⁵⁰, K. Carvalho Akiba^{2,38}, R.C.M. Casanova Mohr³⁶, G. Casse⁵², L. Cassina^{20,k}, L. Castillo Garcia³⁸, M. Cattaneo³⁸, Ch. Cauet⁹, R. Cenci^{23,t}, M. Charles⁸, Ph. Charpentier³⁸, M. Chefdeville⁴, S. Chen⁵⁴, S.-F. Cheung⁵⁵, N. Chiapolini⁴⁰, M. Chrzasczcz^{40,26}, X. Cid Vidal³⁸, G. Ciezarek⁴¹, P.E.L. Clarke⁵⁰, M. Clemencic³⁸, H.V. Cliff⁴⁷, J. Closier³⁸, V. Coco³⁸, J. Cogan⁶, E. Cogneras⁵, V. Cogoni¹⁵, L. Cojocariu²⁹, G. Collazuol²², P. Collins³⁸, A. Comerma-Montells¹¹, A. Contu^{15,38}, A. Cook⁴⁶, M. Coombes⁴⁶, S. Coquereau⁸, G. Corti³⁸, M. Corvo^{16,f}, I. Counts⁵⁶, B. Couturier³⁸, G.A. Cowan⁵⁰, D.C. Craik⁴⁸, A.C. Crocombe⁴⁸, M. Cruz Torres⁶⁰, S. Cunliffe⁵³, R. Currie⁵³, C. D'Ambrosio³⁸, J. Dalseno⁴⁶, P. David⁸, P.N.Y. David⁴¹, A. Davis⁵⁷, K. De Bruyn⁴¹, S. De Capua⁵⁴, M. De Cian¹¹, J.M. De Miranda¹, L. De Paula², W. De Silva⁵⁷, P. De Simone¹⁸, C.-T. Dean⁵¹, D. Decamp⁴, M. Deckenhoff⁹, L. Del Buono⁸, N. Déleage⁴, D. Derkach⁵⁵, O. Deschamps⁵, F. Dettori³⁸, B. Dey⁴⁰, A. Di Canto³⁸, A. Di Domenico²⁵, H. Dijkstra³⁸, S. Donleavy⁵², F. Dordei¹¹, M. Dorigo³⁹, A. Dosil Suárez³⁷, D. Dossett⁴⁸, A. Dovbnya⁴³, K. Dreimanis⁵², G. Dujany⁵⁴, F. Dupertuis³⁹, P. Durante³⁸, R. Dzhelyadin³⁵, A. Dziurda²⁶, A. Dzyuba³⁰, S. Easo^{49,38}, U. Egede⁵³, V. Egorychev³¹, S. Eidelman³⁴, S. Eisenhardt⁵⁰, U. Eitschberger⁹, R. Ekelhof⁹, L. Eklund⁵¹, I. El Rifai⁵, Ch. Elsasser⁴⁰, S. Ely⁵⁹, S. Esen¹¹, H.M. Evans⁴⁷, T. Evans⁵⁵, A. Falabella¹⁴, C. Färber¹¹, C. Farinelli⁴¹, N. Farley⁴⁵, S. Farry⁵², R. Fay⁵², D. Ferguson⁵⁰, V. Fernandez Albor³⁷, F. Ferreira Rodrigues¹, M. Ferro-Luzzi³⁸, S. Filippov³³, M. Fiore^{16,f}, M. Fiorini^{16,f}, M. Firlej²⁷, C. Fitzpatrick³⁹, T. Fiutowski²⁷, P. Fol⁵³, M. Fontana¹⁰, F. Fontanelli^{19,j}, R. Forty³⁸, O. Francisco², M. Frank³⁸, C. Frei³⁸, M. Frosini¹⁷, J. Fu^{21,38}, E. Furfaro^{24,l}, A. Gallas Torreira³⁷, D. Galli^{14,d}, S. Gallorini^{22,38}, S. Gambetta^{19,j}, M. Gandelman², P. Gandini⁵⁹, Y. Gao³, J. García Pardiñas³⁷, J. Garofoli⁵⁹, J. Garra Tico⁴⁷, L. Garrido³⁶, D. Gascon³⁶, C. Gaspar³⁸, U. Gastaldi¹⁶, R. Gauld⁵⁵, L. Gavardi⁹, G. Gazzoni⁵, A. Geraci^{21,v}, E. Gersabeck¹¹, M. Gersabeck⁵⁴, T. Gershon⁴⁸, Ph. Ghez⁴, A. Gianelle²², S. Gianì³⁹, V. Gibson⁴⁷, L. Giubega²⁹, V.V. Gligorov³⁸, C. Göbel⁶⁰, D. Golubkov³¹, A. Golutvin^{53,31,38}, A. Gomes^{1,a}, C. Gotti^{20,k}, M. Grabalosa Gándara⁵, R. Graciani Diaz³⁶, L.A. Granado Cardoso³⁸, E. Graugés³⁶, E. Graverini⁴⁰, G. Graziani¹⁷, A. Greco²⁹, E. Greening⁵⁵, S. Gregson⁴⁷, P. Griffith⁴⁵, L. Grillo¹¹, O. Grünberg⁶³, B. Gui⁵⁹, E. Gushchin³³, Yu. Guz^{35,38}, T. Gys³⁸, C. Hadjivasiliou⁵⁹, G. Haefeli³⁹, C. Haen³⁸, S.C. Haines⁴⁷, S. Hall⁵³, B. Hamilton⁵⁸, T. Hampson⁴⁶, X. Han¹¹, S. Hansmann-Menzemer¹¹, N. Harnew⁵⁵, S.T. Harnew⁴⁶, J. Harrison⁵⁴, J. He³⁸, T. Head³⁹, V. Heijne⁴¹, K. Hennessy⁵², P. Henrard⁵, L. Henry⁸, J.A. Hernando Morata³⁷, E. van Herwijnen³⁸, M. Heß⁶³, A. Hicheur², D. Hill⁵⁵, M. Hoballah⁵, C. Hombach⁵⁴, W. Hulsbergen⁴¹, N. Hussain⁵⁵, D. Hutchcroft⁵², D. Hynds⁵¹, M. Idzik²⁷, P. Ilten⁵⁶, R. Jacobsson³⁸, A. Jaeger¹¹, J. Jalocha⁵⁵, E. Jans⁴¹, P. Jaton³⁹, A. Jawahery⁵⁸, F. Jing³, M. John⁵⁵, D. Johnson³⁸, C.R. Jones⁴⁷, C. Joram³⁸, B. Jost³⁸, N. Jurik⁵⁹, S. Kandybei⁴³, W. Kanso⁶, M. Karacson³⁸, T.M. Karbach³⁸, S. Karodia⁵¹, M. Kelsey⁵⁹, I.R. Kenyon⁴⁵, T. Ketel⁴², B. Khanji^{20,38,k}, C. Khurewathanakul³⁹, S. Klaver⁵⁴, K. Klimaszewski²⁸, O. Kochebina⁷, M. Kolpin¹¹, I. Komarov³⁹, R.F. Koopman⁴², P. Koppenburg^{41,38}, M. Korolev³², L. Kravchuk³³, K. Kreplin¹¹, M. Kreps⁴⁸, G. Krocker¹¹, P. Krokovny³⁴, F. Kruse⁹, W. Kucewicz^{26,o}, M. Kucharczyk^{20,26,k}, V. Kudryavtsev³⁴, K. Kurek²⁸, T. Kvaratskheliya³¹, V.N. La Thi³⁹, D. Lacarrere³⁸, G. Lafferty⁵⁴, A. Lai¹⁵, D. Lambert⁵⁰, R.W. Lambert⁴², G. Lanfranchi¹⁸, C. Langenbruch⁴⁸, B. Langhans³⁸, T. Latham⁴⁸, C. Lazzeroni⁴⁵, R. Le Gac⁶, J. van Leerdam⁴¹, J.-P. Lees⁴, R. Lefèvre⁵, A. Leflat³², J. Lefrançois⁷, O. Leroy⁶, T. Lesiak²⁶, B. Leverington¹¹, Y. Li³, T. Likhomanenko⁶⁴, M. Liles⁵², R. Lindner³⁸, C. Linn³⁸, F. Lionetto⁴⁰, B. Liu¹⁵, S. Lohn³⁸, I. Longstaff⁵¹, J.H. Lopes², P. Lowdon⁴⁰, D. Lucchesi^{22,r}, H. Luo⁵⁰, A. Lupato²², E. Luppi^{16,f}, O. Lupton⁵⁵, F. Machefert⁷, I.V. Machikhiliyan³¹, F. Maciuc²⁹, O. Maev³⁰, S. Malde⁵⁵, A. Malinin⁶⁴, G. Manca^{15,e}, G. Mancinelli⁶, A. Mapelli³⁸,

J. Maratas⁵, J.F. Marchand⁴, U. Marconi¹⁴, C. Marin Benito³⁶, P. Marino^{23,t}, R. Märki³⁹, J. Marks¹¹, G. Martellotti²⁵, M. Martinelli³⁹, D. Martinez Santos⁴², F. Martinez Vidal⁶⁵, D. Martins Tostes², A. Massafferri¹, R. Matev³⁸, Z. Mathe³⁸, C. Matteuzzi²⁰, A. Mazurov⁴⁵, M. McCann⁵³, J. McCarthy⁴⁵, A. McNab⁵⁴, R. McNulty¹², B. McSkelly⁵², B. Meadows⁵⁷, F. Meier⁹, M. Meissner¹¹, M. Merk⁴¹, D.A. Milanes⁶², M.-N. Minard⁴, N. Moggi¹⁴, J. Molina Rodriguez⁶⁰, S. Monteil⁵, M. Morandin²², P. Morawski²⁷, A. Mordà⁶, M.J. Morello^{23,t}, J. Moron²⁷, A.-B. Morris⁵⁰, R. Mountain⁵⁹, F. Muheim⁵⁰, K. Müller⁴⁰, M. Mussini¹⁴, B. Muster³⁹, P. Naik⁴⁶, T. Nakada³⁹, R. Nandakumar⁴⁹, I. Nasteva², M. Needham⁵⁰, N. Neri²¹, S. Neubert³⁸, N. Neufeld³⁸, M. Neuner¹¹, A.D. Nguyen³⁹, T.D. Nguyen³⁹, C. Nguyen-Mau^{39,q}, M. Nicol⁷, V. Niess⁵, R. Niet⁹, N. Nikitin³², T. Nikodem¹¹, A. Novoselov³⁵, D.P. O’Hanlon⁴⁸, A. Oblakowska-Mucha²⁷, V. Obraztsov³⁵, S. Ogilvy⁵¹, O. Okhrimenko⁴⁴, R. Oldeman^{15,e}, C.J.G. Onderwater⁶⁶, M. Orlandea²⁹, J.M. Otalora Goicochea², A. Otto³⁸, P. Owen⁵³, A. Oyanguren⁶⁵, B.K. Pal⁵⁹, A. Palano^{13,c}, F. Palombo^{21,u}, M. Palutan¹⁸, J. Panman³⁸, A. Papanestis^{49,38}, M. Pappagallo⁵¹, L.L. Pappalardo^{16,f}, C. Parkes⁵⁴, C.J. Parkinson^{9,45}, G. Passaleva¹⁷, G.D. Patel⁵², M. Patel⁵³, C. Patrignani^{19,j}, A. Pearce^{54,49}, A. Pellegrino⁴¹, G. Penso^{25,m}, M. Pepe Altarelli³⁸, S. Perazzini^{14,d}, P. Perret⁵, L. Pescatore⁴⁵, E. Pesen⁶⁷, K. Petridis⁵³, A. Petrolini^{19,j}, E. Picatoste Olloqui³⁶, B. Pietrzyk⁴, T. Pilař⁴⁸, D. Pinci²⁵, A. Pistone¹⁹, S. Playfer⁵⁰, M. Plo Casasus³⁷, F. Polci⁸, A. Poluektov^{48,34}, I. Polyakov³¹, E. Polycarpo², A. Popov³⁵, D. Popov¹⁰, B. Popovici²⁹, C. Potterat², E. Price⁴⁶, J.D. Price⁵², J. Prisciandaro³⁹, A. Pritchard⁵², C. Prouve⁴⁶, V. Pugatch⁴⁴, A. Puig Navarro³⁹, G. Punzi^{23,s}, W. Qian⁴, B. Rachwal²⁶, J.H. Rademacker⁴⁶, B. Rakotomiaramananana³⁹, M. Rama²³, M.S. Rangel², I. Raniuk⁴³, N. Rauschmayr³⁸, G. Raven⁴², F. Redi⁵³, S. Reichert⁵⁴, M.M. Reid⁴⁸, A.C. dos Reis¹, S. Ricciardi⁴⁹, S. Richards⁴⁶, M. Rihl³⁸, K. Rinnert⁵², V. Rives Molina³⁶, P. Robbe⁷, A.B. Rodrigues¹, E. Rodrigues⁵⁴, P. Rodriguez Perez⁵⁴, S. Roiser³⁸, V. Romanovsky³⁵, A. Romero Vidal³⁷, M. Rotondo²², J. Rouvinet³⁹, T. Ruf³⁸, H. Ruiz³⁶, P. Ruiz Valls⁶⁵, J.J. Saborido Silva³⁷, N. Sagidova³⁰, P. Sail⁵¹, B. Saitta^{15,e}, V. Salustino Guimaraes², C. Sanchez Mayordomo⁶⁵, B. Sanmartin Sedes³⁷, R. Santacesaria²⁵, C. Santamarina Rios³⁷, E. Santovetti^{24,l}, A. Sarti^{18,m}, C. Satriano^{25,n}, A. Satta²⁴, D.M. Saunders⁴⁶, D. Savrina^{31,32}, M. Schiller³⁸, H. Schindler³⁸, M. Schlupp⁹, M. Schmelling¹⁰, B. Schmidt³⁸, O. Schneider³⁹, A. Schopper³⁸, M.-H. Schune⁷, R. Schwemmer³⁸, B. Sciascia¹⁸, A. Sciubba^{25,m}, A. Semennikov³¹, I. Sepp⁵³, N. Serra⁴⁰, J. Serrano⁶, L. Sestini²², P. Seyfert¹¹, M. Shapkin³⁵, I. Shapoval^{16,43,f}, Y. Shcheglov³⁰, T. Shears⁵², L. Shekhtman³⁴, V. Shevchenko⁶⁴, A. Shires⁹, R. Silva Coutinho⁴⁸, G. Simi²², M. Sirendi⁴⁷, N. Skidmore⁴⁶, I. Skillicorn⁵¹, T. Skwarnicki⁵⁹, N.A. Smith⁵², E. Smith^{55,49}, E. Smith⁵³, J. Smith⁴⁷, M. Smith⁵⁴, H. Snoek⁴¹, M.D. Sokoloff⁵⁷, F.J.P. Soler⁵¹, F. Soomro³⁹, D. Souza⁴⁶, B. Souza De Paula², B. Spaan⁹, P. Spradlin⁵¹, S. Sridharan³⁸, F. Stagni³⁸, M. Stahl¹¹, S. Stahl¹¹, O. Steinkamp⁴⁰, O. Stenyakin³⁵, F. Sterpka⁵⁹, S. Stevenson⁵⁵, S. Stoica²⁹, S. Stone⁵⁹, B. Storaci⁴⁰, S. Stracka^{23,t}, M. Straticiu²⁹, U. Straumann⁴⁰, R. Stroili²², L. Sun⁵⁷, W. Sutcliffe⁵³, K. Swientek²⁷, S. Swientek⁹, V. Syropoulos⁴², M. Szczekowski²⁸, P. Szczypka^{39,38}, T. Szumlak²⁷, S. T’Jampens⁴, M. Teklishyn⁷, G. Tellarini^{16,f}, F. Teubert³⁸, C. Thomas⁵⁵, E. Thomas³⁸, J. van Tilburg⁴¹, V. Tisserand⁴, M. Tobin³⁹, J. Todd⁵⁷, S. Tolk⁴², L. Tomassetti^{16,f}, D. Tonelli³⁸, S. Topp-Joergensen⁵⁵, N. Torr⁵⁵, E. Tournefier⁴, S. Tourneur³⁹, M.T. Tran³⁹, M. Tresch⁴⁰, A. Trisovic³⁸, A. Tsaregorodtsev⁶, P. Tsopelas⁴¹, N. Tuning⁴¹, M. Ubeda Garcia³⁸, A. Ukleja²⁸, A. Ustyuzhanin⁶⁴, U. Uwer¹¹, C. Vacca¹⁵, V. Vagnoni¹⁴, G. Valenti¹⁴, A. Vallier⁷, R. Vazquez Gomez¹⁸, P. Vazquez Regueiro³⁷, C. Vázquez Sierra³⁷, S. Vecchi¹⁶, J.J. Velthuis⁴⁶, M. Veltri^{17,h}, G. Veneziano³⁹, M. Vesterinen¹¹, J.V. Viana Barbosa³⁸, B. Viaud⁷, D. Vieira², M. Vieites Diaz³⁷, X. Vilasis-Cardona^{36,p}, A. Vollhardt⁴⁰, D. Volynskyy¹⁰, D. Voong⁴⁶, A. Vorobyev³⁰, V. Vorobyev³⁴, C. Voß⁶³, J.A. de Vries⁴¹, R. Waldi⁶³, C. Wallace⁴⁸, R. Wallace¹², J. Walsh²³, S. Wandernoth¹¹, J. Wang⁵⁹, D.R. Ward⁴⁷, N.K. Watson⁴⁵, D. Websdale⁵³, M. Whitehead⁴⁸, D. Wiedner¹¹, G. Wilkinson^{55,38}, M. Wilkinson⁵⁹, M.P. Williams⁴⁵, M. Williams⁵⁶, H.W. Wilschut⁶⁶, F.F. Wilson⁴⁹, J. Wimberley⁵⁸, J. Wishahi⁹, W. Wislicki²⁸, M. Witek²⁶, G. Wormser⁷, S.A. Wotton⁴⁷, S. Wright⁴⁷, K. Wyllie³⁸, Y. Xie⁶¹, Z. Xing⁵⁹, Z. Xu³⁹, Z. Yang³, X. Yuan³, O. Yushchenko³⁵, M. Zangoli¹⁴, M. Zavertyaev^{10,b}, L. Zhang³, W.C. Zhang¹², Y. Zhang³, A. Zhelezov¹¹, A. Zhokhov³¹, L. Zhong³

¹ Centro Brasileiro de Pesquisas Físicas (CBPF), Rio de Janeiro, Brazil² Universidade Federal do Rio de Janeiro (UFRJ), Rio de Janeiro, Brazil³ Center for High Energy Physics, Tsinghua University, Beijing, China⁴ LAPP, Université de Savoie, CNRS/IN2P3, Annecy-Le-Vieux, France

- ⁵ Clermont Université, Université Blaise Pascal, CNRS/IN2P3, LPC, Clermont-Ferrand, France
⁶ CPPM, Aix-Marseille Université, CNRS/IN2P3, Marseille, France
⁷ LAL, Université Paris-Sud, CNRS/IN2P3, Orsay, France
⁸ LPNHE, Université Pierre et Marie Curie, Université Paris Diderot, CNRS/IN2P3, Paris, France
⁹ Fakultät Physik, Technische Universität Dortmund, Dortmund, Germany
¹⁰ Max-Planck-Institut für Kernphysik (MPIK), Heidelberg, Germany
¹¹ Physikalisches Institut, Ruprecht-Karls-Universität Heidelberg, Heidelberg, Germany
¹² School of Physics, University College Dublin, Dublin, Ireland
¹³ Sezione INFN di Bari, Bari, Italy
¹⁴ Sezione INFN di Bologna, Bologna, Italy
¹⁵ Sezione INFN di Cagliari, Cagliari, Italy
¹⁶ Sezione INFN di Ferrara, Ferrara, Italy
¹⁷ Sezione INFN di Firenze, Firenze, Italy
¹⁸ Laboratori Nazionali dell'INFN di Frascati, Frascati, Italy
¹⁹ Sezione INFN di Genova, Genova, Italy
²⁰ Sezione INFN di Milano Bicocca, Milano, Italy
²¹ Sezione INFN di Milano, Milano, Italy
²² Sezione INFN di Padova, Padova, Italy
²³ Sezione INFN di Pisa, Pisa, Italy
²⁴ Sezione INFN di Roma Tor Vergata, Roma, Italy
²⁵ Sezione INFN di Roma La Sapienza, Roma, Italy
²⁶ Henryk Niewodniczanski Institute of Nuclear Physics Polish Academy of Sciences, Kraków, Poland
²⁷ AGH – University of Science and Technology, Faculty of Physics and Applied Computer Science, Kraków, Poland
²⁸ National Center for Nuclear Research (NCBJ), Warsaw, Poland
²⁹ Horia Hulubei National Institute of Physics and Nuclear Engineering, Bucharest-Magurele, Romania
³⁰ Petersburg Nuclear Physics Institute (PNPI), Gatchina, Russia
³¹ Institute of Theoretical and Experimental Physics (ITEP), Moscow, Russia
³² Institute of Nuclear Physics, Moscow State University (SINP MSU), Moscow, Russia
³³ Institute for Nuclear Research of the Russian Academy of Sciences (INR RAN), Moscow, Russia
³⁴ Budker Institute of Nuclear Physics (SB RAS) and Novosibirsk State University, Novosibirsk, Russia
³⁵ Institute for High Energy Physics (IHEP), Protvino, Russia
³⁶ Universitat de Barcelona, Barcelona, Spain
³⁷ Universidad de Santiago de Compostela, Santiago de Compostela, Spain
³⁸ European Organization for Nuclear Research (CERN), Geneva, Switzerland
³⁹ Ecole Polytechnique Fédérale de Lausanne (EPFL), Lausanne, Switzerland
⁴⁰ Physik-Institut, Universität Zürich, Zürich, Switzerland
⁴¹ Nikhef National Institute for Subatomic Physics, Amsterdam, The Netherlands
⁴² Nikhef National Institute for Subatomic Physics and VU University Amsterdam, Amsterdam, The Netherlands
⁴³ NSC Kharkiv Institute of Physics and Technology (NSC KIPT), Kharkiv, Ukraine
⁴⁴ Institute for Nuclear Research of the National Academy of Sciences (KINR), Kyiv, Ukraine
⁴⁵ University of Birmingham, Birmingham, United Kingdom
⁴⁶ H.H. Wills Physics Laboratory, University of Bristol, Bristol, United Kingdom
⁴⁷ Cavendish Laboratory, University of Cambridge, Cambridge, United Kingdom
⁴⁸ Department of Physics, University of Warwick, Coventry, United Kingdom
⁴⁹ STFC Rutherford Appleton Laboratory, Didcot, United Kingdom
⁵⁰ School of Physics and Astronomy, University of Edinburgh, Edinburgh, United Kingdom
⁵¹ School of Physics and Astronomy, University of Glasgow, Glasgow, United Kingdom
⁵² Oliver Lodge Laboratory, University of Liverpool, Liverpool, United Kingdom
⁵³ Imperial College London, London, United Kingdom
⁵⁴ School of Physics and Astronomy, University of Manchester, Manchester, United Kingdom
⁵⁵ Department of Physics, University of Oxford, Oxford, United Kingdom
⁵⁶ Massachusetts Institute of Technology, Cambridge, MA, United States
⁵⁷ University of Cincinnati, Cincinnati, OH, United States
⁵⁸ University of Maryland, College Park, MD, United States
⁵⁹ Syracuse University, Syracuse, NY, United States
⁶⁰ Pontifícia Universidade Católica do Rio de Janeiro (PUC-Rio), Rio de Janeiro, Brazil^w
⁶¹ Institute of Particle Physics, Central China Normal University, Wuhan, Hubei, China^x
⁶² Departamento de Física, Universidad Nacional de Colombia, Bogotá, Colombia^y
⁶³ Institut für Physik, Universität Rostock, Rostock, Germany^z
⁶⁴ National Research Centre Kurchatov Institute, Moscow, Russia^{aa}
⁶⁵ Instituto de Física Corpuscular (IFIC), Universitat de Valencia-CSIC, Valencia, Spain^{ab}
⁶⁶ Van Swinderen Institute, University of Groningen, Groningen, The Netherlands^{ac}
⁶⁷ Celal Bayar University, Manisa, Turkey^{ad}

* Corresponding author.

E-mail address: Ivan.Belyaev@itep.ru (I. Belyaev).

^a Universidade Federal do Triângulo Mineiro (UFTM), Uberaba-MG, Brazil.

^b P.N. Lebedev Physical Institute, Russian Academy of Science (LPI RAS), Moscow, Russia.

^c Università di Bari, Bari, Italy.

^d Università di Bologna, Bologna, Italy.

^e Università di Cagliari, Cagliari, Italy.

^f Università di Ferrara, Ferrara, Italy.

^g Università di Firenze, Firenze, Italy.

^h Università di Urbino, Urbino, Italy.

ⁱ Università di Modena e Reggio Emilia, Modena, Italy.

^j Università di Genova, Genova, Italy.

^k Università di Milano Bicocca, Milano, Italy.

- ^l Università di Roma Tor Vergata, Roma, Italy.
- ^m Università di Roma La Sapienza, Roma, Italy.
- ⁿ Università della Basilicata, Potenza, Italy.
- ^o AGH – University of Science and Technology, Faculty of Computer Science, Electronics and Telecommunications, Kraków, Poland.
- ^p LIFAELS, La Salle, Universitat Ramon Llull, Barcelona, Spain.
- ^q Hanoi University of Science, Hanoi, Viet Nam.
- ^r Università di Padova, Padova, Italy.
- ^s Università di Pisa, Pisa, Italy.
- ^t Scuola Normale Superiore, Pisa, Italy.
- ^u Università degli Studi di Milano, Milano, Italy.
- ^v Politecnico di Milano, Milano, Italy.
- ^w Associated to Universidade Federal do Rio de Janeiro (UFRJ), Rio de Janeiro, Brazil.
- ^x Associated to Center for High Energy Physics, Tsinghua University, Beijing, China.
- ^y Associated to LPNHE, Université Pierre et Marie Curie, Université Paris Diderot, CNRS/IN2P3, Paris, France.
- ^z Associated to Physikalisches Institut, Ruprecht-Karls-Universität Heidelberg, Heidelberg, Germany.
- ^{aa} Associated to Institute of Theoretical and Experimental Physics (ITEP), Moscow, Russia.
- ^{ab} Associated to Universitat de Barcelona, Barcelona, Spain.
- ^{ac} Associated to Nikhef National Institute for Subatomic Physics, Amsterdam, The Netherlands.
- ^{ad} Associated to European Organization for Nuclear Research (CERN), Geneva, Switzerland.